# Spemann organizer gene *Goosecoid* promotes delamination of neuroblasts from the otic vesicle

Husniye Kantarci[a], Andrea Gerberding[a], and Bruce B. Riley[a,1]

[a]Biology Department, Texas A&M University, College Station, TX 77843-3258

Edited by Marianne Bronner, California Institute of Technology, Pasadena, CA, and approved September 23, 2016 (received for review June 6, 2016)

**Neurons of the Statoacoustic Ganglion (SAG), which innervate the inner ear, originate as neuroblasts in the floor of the otic vesicle and subsequently delaminate and migrate toward the hindbrain before completing differentiation. In all vertebrates, locally expressed Fgf initiates SAG development by inducing expression of *Neurogenin1* (*Ngn1*) in the floor of the otic vesicle. However, not all Ngn1-positive cells undergo delamination, nor has the mechanism controlling SAG delamination been elucidated. Here we report that *Goosecoid* (*Gsc*), best known for regulating cellular dynamics in the Spemann organizer, regulates delamination of neuroblasts in the otic vesicle. In zebrafish, Fgf coregulates expression of *Gsc* and Ngn1 in partially overlapping domains, with delamination occurring primarily in the zone of overlap. Loss of Gsc severely inhibits delamination, whereas overexpression of Gsc greatly increases delamination. Comisexpression of Ngn1 and *Gsc* induces ectopic delamination of some cells from the medial wall of the otic vesicle but with a low incidence, suggesting the action of a local inhibitor. The medial marker Pax2a is required to restrict the domain of *gsc* expression, and misexpression of Pax2a is sufficient to block delamination and fully suppress the effects of *Gsc*. The opposing activities of *Gsc* and Pax2a correlate with repression or up-regulation, respectively, of E-cadherin (*cdh1*). These data resolve a genetic mechanism controlling delamination of otic neuroblasts. The data also elucidate a developmental role for *Gsc* consistent with a general function in promoting epithelial-to-mesenchymal transition (EMT).**

inner ear | neurogenesis | EMT | *Gsc* | Pax2

The Statoacoustic Ganglion (SAG) connects the inner ear to the brain and transmits hearing and balance information. SAG neurons are generated by a stepwise program that starts in the otic vesicle, the precursor of the inner ear. Initially, a subset of the cells in the otic epithelium is specified for neural fate by the up-regulation of the proneural gene *neurogenin1* (*ngn1*) (1, 2). Otic expression of *ngn1* is first detected by 16 hpf, peaks at around 24 hours postfertilization (hpf), and then gradually declines, ceasing entirely by 42 hpf (3). Throughout this period, a subset of newly specified neuroblasts undergoes epithelial-to-mesenchymal transition (EMT) and delaminates from the otic vesicle (4–6). In zebrafish, most neuroblasts lose *ngn1* expression after leaving the otic vesicle and subsequently up-regulate the related proneural factor *neurod* (7, 8). *neurod*-expressing cells form a group of proliferating and migrating precursors called the transit-amplifying (TA) pool (3, 9). As TA cells differentiate into mature SAG neurons, they lose *neurod* expression and up-regulate mature neuronal markers such as Islet1 and Islet2b (10, 11). The first mature Isl1+ SAG neurons are detected by 20 hpf and subsequently accumulate at a linear rate through at least 72 hpf (3). At the same time, the TA pool is maintained as a stable population by proliferative renewal, assuring further growth of the SAG as larvae develop (3).

Specification of the neurogenic domain is established by a low threshold level of Fgf signaling (3, 12). However, nothing is known about the mechanisms regulating delamination of neuroblasts from the otic vesicle. Ngn1 is required for neuroblast fate specification (1, 2), but *ngn1* is not sufficient to induce delamination. In mouse, many cells that initially express *Ngn1* ultimately remain in the otic vesicle and contribute to developing sensory epithelia (13). In zebrafish too, delamination of cells within the *ngn1* domain appears highly restricted. Clearly additional factors are required to initiate EMT in the otic epithelium during SAG development.

In addition to positive regulation, other factors appear to stabilize the otic epithelium and prevent inappropriate EMT. In zebrafish, chick, and mouse, Pax2 marks the nascent otic placode and is later restricted to the medial half of the otic vesicle (14–18). Loss of Pax2 and related factor Pax8 compromises epithelial integrity, leading to faulty morphogenesis of the otic vesicle and cell dispersal (17, 18).

EMT is characterized by loss of epithelial markers and up-regulation of mesenchymal genes, many of which confer the ability to migrate. This process is critical for establishment of the vertebrate body plan during gastrulation and is initiated by a unique group of cells originally described as Spemann's organizer. *Goosecoid* (*gsc*) is the most abundantly expressed homeobox gene in the vertebrate organizer (19, 20). Ectopic expression of *Gsc* is sufficient to induce organizer activity (21) and promote cell migration (22). *Gsc* is also expressed in the tissues that undergo tissue remodeling at later stages, such as neural crest-derived mesenchymal tissues (23). Loss of *Gsc* function leads to craniofacial defects in mouse and humans (24–26). It has also been found that many aggressive metastatic cancers show strong up-regulation of *Gsc*, and experimental misexpression of *Gsc* strongly promotes EMT and enhances metastasis (27, 28). Interestingly, *Gsc* expression has been reported in the developing otic vesicle in mouse (23, 29), but its functional importance has never been investigated. Due to these widespread roles of *Gsc* in regulating

## Significance

**Neurons that innervate the inner ear originate as neuroblasts in the otic vesicle, the epithelial precursor of the inner ear. Neuroblasts subsequently delaminate from the otic epithelium to complete differentiation near the hindbrain. Despite growing understanding of otic neurogenesis, the mechanism by which neuroblasts delaminate from the otic vesicle is unknown. Here we show that delamination is triggered by *Goosecoid* (*Gsc*), a homeobox gene famously discovered as the first known regulator of the "Spemann" embryonic organizer. *Gsc* is expressed in the otic vesicle in a region overlapping with neuroblasts, inducing localized epithelial-to-mesenchymal transition (EMT). Hence, regulation of cellular dynamics appears to be a general function of *Gsc* during otic neurogenesis as well as in the embryonic organizer.**

Author contributions: H.K. and B.B.R. designed research; H.K. and A.G. performed research; H.K., A.G., and B.B.R. analyzed data; and H.K. and B.B.R. wrote the paper.

The authors declare no conflict of interest.

This article is a PNAS Direct Submission.

[1]To whom correspondence should be addressed. Email: briley@bio.tamu.edu.

This article contains supporting information online at www.pnas.org/lookup/suppl/doi:10.1073/pnas.1609146113/-/DCSupplemental.

epithelial dynamics, we examined whether *Gsc* regulates EMT during otic neurogenesis in zebrafish.

Here we describe a full time course for *gsc* expression in the zebrafish otic vesicle. Disruption of gsc impairs delamination of SAG neuroblasts, whereas misexpression of gsc strongly promotes neuroblast delamination. Although *gsc* is regulated by Fgf in a domain that partially overlaps with *ngn1*, *gsc* does not affect neural fate specification. Thus, *ngn1* and *gsc* act in parallel downstream of Fgf to coordinate neural fate specification with morphogenesis. Further analysis revealed the transcription factor Pax2a functions as a strong epithelializing factor expressed in the nonneurogenic regions of the otic vesicle. Moreover, Pax2a represses *gsc* transcription and function, helping to restrict EMT to the neurogenic domain of the otic vesicle.

## Results

**Expression of *gsc* During Otic Neurogenesis.** To assess the function of *gsc* during development of SAG neurons, we examined expression of *gsc* in the otic vesicle during relevant stages. *gsc* is first detected in a small number of ventral otic cells at 20 hpf and becomes strongly up-regulated in a ventrolateral domain by 22 hpf (Fig. 1 *A* and *B*). This domain lies close to the neurogenic domain of the otic vesicle (1). Ventrolateral expression of *gsc* is maintained in the otic vesicle through at least 48 hpf (Fig. 1 *C*–*F*), beyond the stage when neurogenesis normally ceases (3).

Neurogenesis in the otic vesicle, marked by expression of *ngn1*, is initiated by a low level of Fgf signaling, whereas high-level Fgf signaling blocks expression of *ngn1* (3). Expression of *gsc* shows similar regulation by Fgf. Specifically, blocking Fgf signaling by activation of *hs:dnfgfr1* (dominant-negative Fgf receptor) completely eliminated *gsc* expression in the otic vesicle (Fig. 1 *G* and *H*). Additionally, low-level activation of *hs:fgf8* at 35 °C expanded the domain of *gsc* expression, with a more modest expansion seen at 37 °C (Fig. 1 *I* and *J*). Thus, the requirement for Fgf and response to low-level Fgf appears highly similar for *gsc* and *ngn1*. However, expression of *gsc* does not require *ngn1*: High-level activation of *hs:fgf8* at 39 °C represses *ngn1* expression (3) but did not abolish *gsc* expression (Fig. 1*K*). Additionally, expression of *gsc* was normal in *ngn1* morphants (Fig. 1*L*). Similarly, *ngn1* expression does not require *gsc* (Fig. 2*B*). Thus, *gsc* and *ngn1* are coinduced by low-level Fgf signaling but are not dependent on each other.

We next compared the spatial patterns of *gsc* and *ngn1* expression in serial sections. This confirmed that expression of *gsc* partially overlaps with *ngn1* in the otic floor at least through 36 hpf (Fig. 1 *M*–*R*). *gsc* expression can also be detected in a small number of cells just ventral to the otic vesicle (Fig. 1*M*), presumably marking recently delaminated neuroblasts. After leaving the otic vesicle, these cells quickly lose *gsc* expression: Neither TA neuroblasts (marked by *neurod*) nor mature SAG neurons (marked by Isl1) show detectable expression of *gsc* (Fig. S1). To further examine the degree of overlap between *gsc* and *ngn1* expression domains, we mapped the locations of cells expressing either *gsc* or *ngn1* in the otic floor based on data from serial sections. *ngn1* is expressed in the otic floor adjacent and lateral to the developing sensory epithelia (Fig. 1*S*). Expression of *gsc* overlaps with lateral portions of the *ngn1* domain but extends to more lateral and posterior regions of the otic floor (Fig. 1*S*). Because *Gsc* is known to regulate EMT (22, 28), we also examined expression of GM130, a Golgi marker that undergoes a dramatic basal relocalization as cells undergo EMT (30, 31). The pattern of GM130 staining in the otic floor revealed that the highest rate of EMT occurs in the region where *ngn1* and *gsc* are coexpressed (Fig. 1*S*).

**Role of Gsc During Otic Neurogenesis.** We next tested the effects of disrupting or misexpressing *gsc* on otic neurogenesis. Using transcription activator-like effector nuclease (TALEN)-mediated targeting,

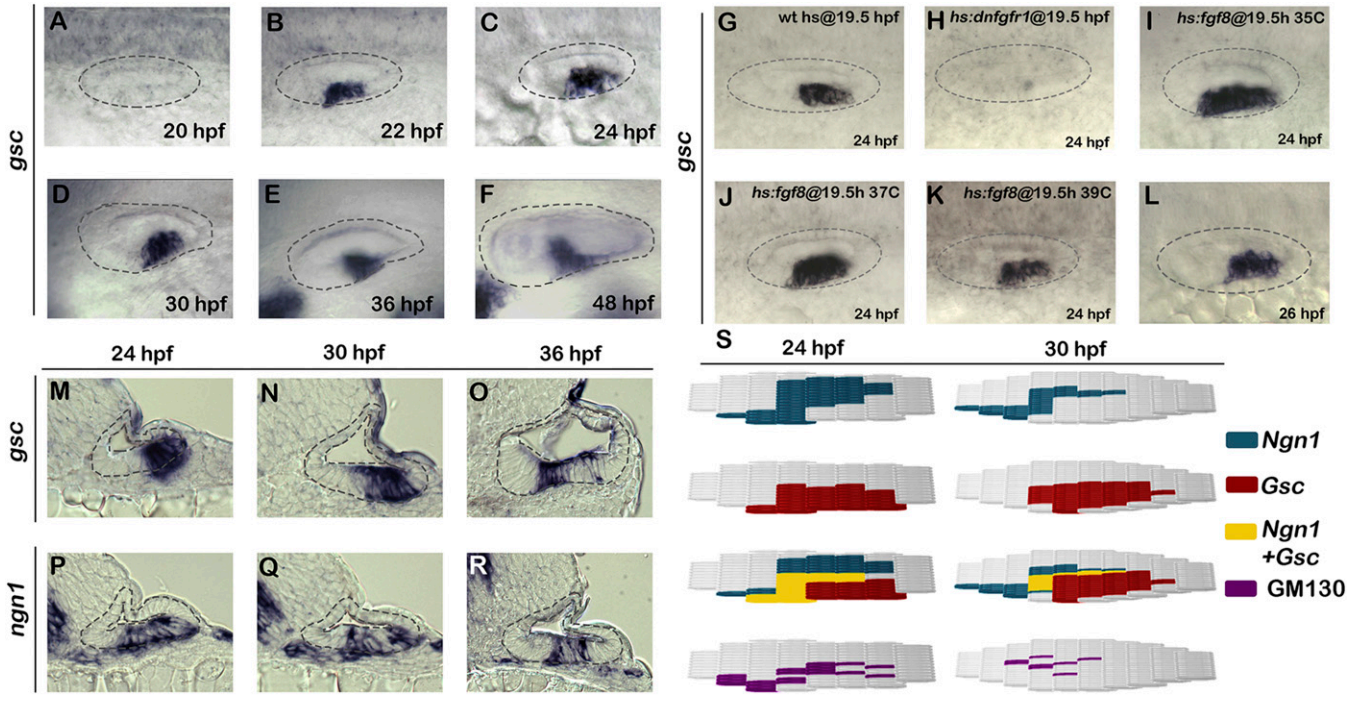


**Fig. 1.** Expression and regulation of *gsc* during otic neurogenesis. (*A*–*L*) Whole-mount images (dorsal up, anterior left) show dorsolateral views of *gsc* expression in the otic vesicle (outlined) at the indicated times. (*M*–*R*) Cross-sections (dorsal up, medial left) passing through the widest part of the neurogenic domain showing expression of *gsc* or *ngn1* at the indicated times. The otic epithelium is outlined in each image. (Magnification: *F*, 512×; all other images, 640×.) (*S*) Maps of regional markers in the floor of the otic vesicle (medial up, anterior left) generated from serial cross-sections of embryos stained for *ngn1*, *gsc*, or GM130 at 24 or 30 hpf. The location and number of cells expressing individual markers (four embryos each) was normalized and plotted accordingly.

we recovered two lesions predicted to eliminate *gsc* function (Fig. S2*A*). Disruption of *gsc* did not cause axial defects or any overt changes in the gross morphology at 24 hpf (Fig. S2 *B* and *C*). However, *gsc* mutants did show a slight (~7%) reduction in the size of the otic vesicle (Fig. S2 *G–I* and *N*) and impaired neural delamination (Fig. 2*G*). At later stages, *gsc* mutants also developed cardiac edema and a severe jaw defect (Fig. S2 *J–M*). Similar phenotypes were seen in *gsc* morphants, although *gsc* morphants also showed mild brain necrosis not observed in mutant embryos (Fig. S2 *D–F*).

Despite the reduced size of the otic vesicle in *gsc* mutants, most aspects of otic patterning appeared normal, including expression of various regional markers and accumulation of sensory hair cells (Fig. S3). In addition, *gsc* mutants produced a normal number of the *ngn1*+ neuroblasts in the otic epithelium (Fig. 2 *A*, *B*, and *G*). However, the number of *ngn1*+ neuroblasts outside the otic vesicle was reduced by more than 50% at all stages of neurogenesis, suggesting a reduced rate of neuroblast delamination. A similar deficiency of recently delaminated *ngn1*+ neuroblasts was seen in *gsc* morphants (Fig. 2*G*).

To overexpress *gsc*, we generated a heat shock-inducible transgenic line, *hs:gsc* (Fig. S4). Overexpression of *gsc* at 22 hpf led to a dramatic decrease in the number of *ngn1*+ neuroblasts in the otic epithelium within 60 min, with a concomitant increase in the number of *ngn1*+ cells outside the otic vesicle (Fig. 2 *C*, *H*, and *I*). The number of *ngn1*+ cells outside the ear remained elevated in *hs:gsc* embryos for several hours but then returned to control levels by 25 hpf (Fig. 2*I*), presumably reflecting the decline in transgene activity (Fig. S4). Activation of *hs:gsc* at 30 hpf or 36 hpf gave results similar to those observed following activation at 22 hpf (Fig. 2 *H* and *I*). Otic neurogenesis normally ends by 42 hpf (3), so we tested whether activation of *hs:gsc* at this stage could reinitiate neuroblast specification. Activation of *hs:gsc* at 42 hpf failed to reinitiate *ngn1* expression in the otic vesicle but nevertheless caused a substantial increase in the number of *ngn1*+ cells outside the otic vesicle (Fig. 2 *D*, *F*, *H*, and *I*). This latter increase appears to result from a stage-specific effect on proliferation of TA neuroblasts (Fig. 3*K*). Together, these data suggest that *Gsc* does not affect neuroblast specification but instead enhances the ability of neuroblasts to leave the

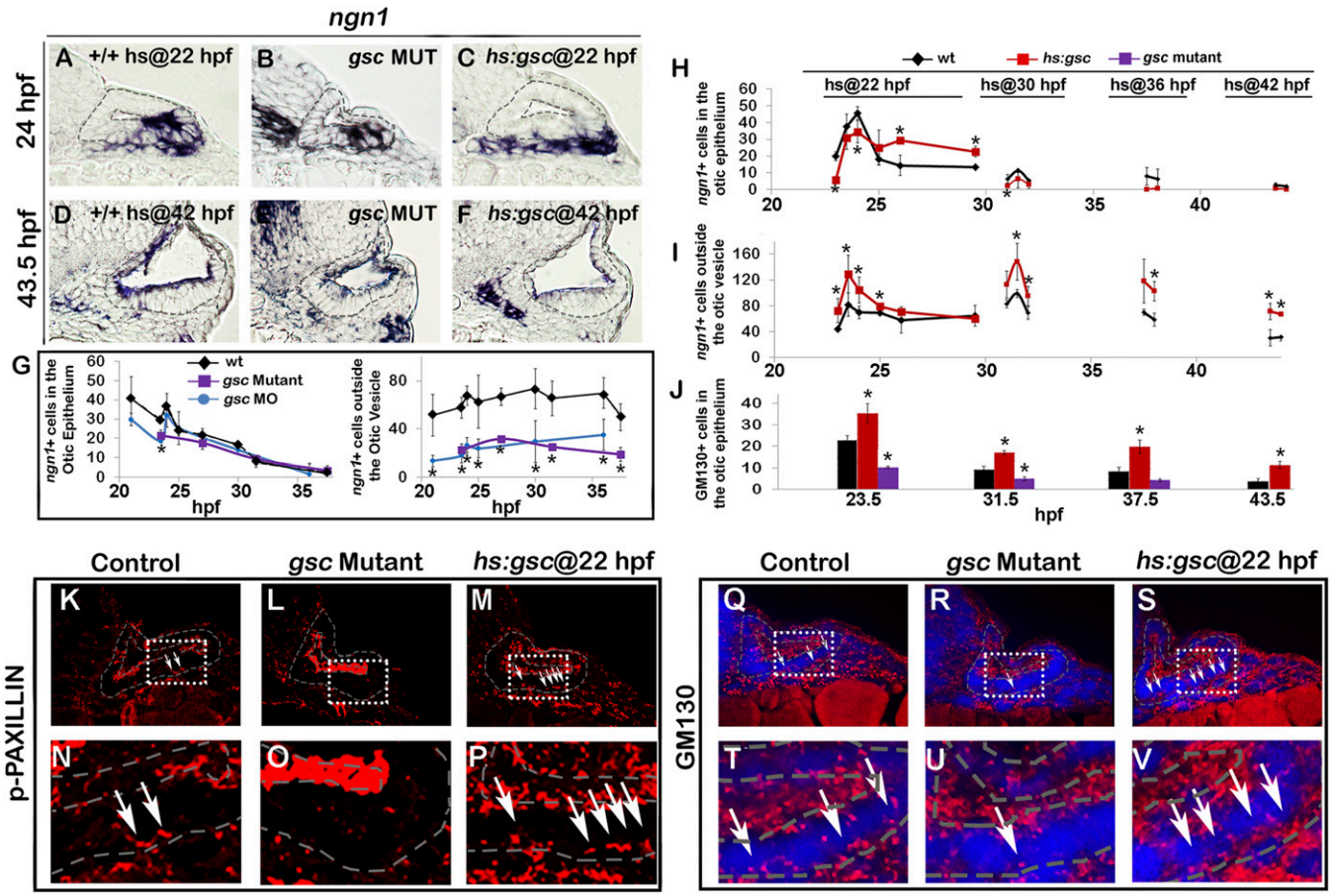


**Fig. 2.** *Gsc* promotes EMT of otic neuroblasts. (*A–F*) Expression of *ngn1* in cross-sections passing through the widest part of the neurogenic domain (dorsal up, medial left) just posterior to the utricular sensory epithelium expression in controls, *gsc* mutants, and *hs:gsc* embryos at 24 hpf (*A–C*) or 43.5 hpf (*D–F*). Control and transgenic embryos were heat shocked at 22 hpf (*A* and *C*) or 42 hpf (*D* and *F*). The otic epithelium is outlined in each image. (*G*) Mean and SD of the total number of *ngn1*+ cells in the otic epithelium and outside the otic vesicle for the genotypes indicated in the color key (counted from the serial sections, $n = 3$ or 4 otic vesicles per time point). The number of *ngn1*+ neuroblasts in the otic epithelium was normal in *gsc* mutants and morphants at all stages, except for a small but significant reduction seen in *gsc* morphants at 24 hpf ($P < 0.05$, asterisk). (*H–J*) For the genotypes indicated in the color key, embryos were heat shocked at the indicated times and fixed several hours later to stain for *ngn1* (*H* and *I*) or basal relocalization of GM130 (*J*). Data show the mean and SD of the total number of stained cells in the otic epithelium or delaminated cells outside the otic vesicle (counted from the serial sections, $n = 3$ otic vesicles per time point). Asterisks indicate significant differences from control specimens ($P < 0.05$). (*K–V*) EMT markers in cross-sections (dorsal up, anterior left) passing through the neurogenic domain of control embryos, *gsc* mutants, or *hs:gsc* embryos immunostained for p-Paxillin (*K–P*) or GM130 (red) and DAPI (blue) (*Q–V*). Controls and transgenic embryos were heat shocked at 22 hpf. Boxed regions in *K–M* are magnified in *N–P*, and boxed regions in *Q–S* are magnified in *T–V*. White arrows indicate elevated basal staining in cells undergoing EMT. (Magnification: *A*, *B*, *D*, *E*, *K–M*, *Q–S*, 640×; *C* and *F*, 512×; *N–P*, *T–V*, 2,000×.)

otic vesicle. The effect of *Gsc* on neuroblast delamination was highly specific, as other aspects of otic vesicle development appeared largely normal several hours after activating *hs:gsc* (Fig. S3).

We next examined the effects of Gsc on the epithelial and mesenchymal cell markers. Zonula Occludens (ZO)-1 is expressed apically in epithelial otic cells but is lost upon transition to the mesenchymal state (Fig. S5 *A*, *D*, and *G*), whereas the transition is marked by activation of the focal adhesion protein p-Paxillin at the leading edge of migrating cells (Fig. 2 *K* and *N* and Fig. S5*A*). Delaminating otic cells also show dramatic redistribution of golgi marker GM130 to the basal surface as cells transition to the mesenchymal state (Fig. 2 *Q* and *T*). *Gsc* mutants showed more ZO-1 staining in the otic epithelium (Fig. S5 *B*, *E*, and *H*) and a loss of cells with p-Paxillin staining (Fig. 2 *L* and *O*). *gsc* mutants also showed a reduced number of cells with basal GM130 staining (Fig. 2 *R* and *U*). Conversely, activation of *hs:gsc* reduced the ZO-1 staining in the otic epithelium (Fig. S5 *C*, *F*, and *I*) and increased the number of cells with p-Paxillin staining (Fig. 2 *M* and *P* and Fig. S5*C*). Activation of *hs:gsc* also increased the number of cells with basal GM130 staining (Fig. 2 *S* and *V*). Overall, these results suggest that *gsc* stimulates EMT of neural progenitors in the otic vesicle without affecting cell fate specification. Consistent with this idea, we observed a ∼12% decrease in the size of the otic vesicle at 24 hpf following activation of *hs:gsc* at 22 hpf (Fig. S6 *A* and *D*), likely caused by the increased number of cells leaving the otic vesicle. This size reduction persisted through at least 31 hpf (Fig. S6), suggesting a limited capacity to compensate for earlier cell loss.

**Effects of *Gsc* on Later Stages of SAG Development.** Next, we examined whether altered delamination of neuroblasts affected later stages of neural development. Normally, newly delaminated neural progenitors quickly lose expression of *ngn1* and up-regulate *neurod*, marking the TA stage of SAG development (3, 7–9). TA cells migrate toward the hindbrain as they proliferate and then differentiate into mature neurons, marked by Isl1 staining. The number of *neurod*+ TA cells and mature neurons was significantly reduced in *gsc* mutants and morphants at every time point examined (Fig. 3 *B*, *E*, *G*, and *H*). This is consistent with impairment of neuroblast delamination seen in these embryos. Conversely, activation of *hs:gsc* at 22 hpf led to a ∼30% increase in the number of *neurod*+ TA cells and mature neurons (Fig. 3 *C* and *F*–*H*). Furthermore, the number of mature SAG neurons remained elevated in these embryos through at least 50 hpf before returning to control levels (Fig. 3*H*). Overexpression of *gsc* during earlier placodal stages also increased accumulation of Isl1+ neurons at 30 hpf, although to a lesser degree than activation at 22 hpf (Fig. S7*C*). Activation of *hs:gsc* at 30 hpf gave results similar to activation at 22 hpf (Fig. 3 *I* and *J* and Fig. S7 *A* and *B*). Interestingly, activation of *hs:gsc* at 36 or 42 hpf caused a disproportionately greater increase in the number of *neurod*+ TA cells compared with earlier activation (Fig. 3*I*). This was unexpected because rates of neuroblast specification are very low at these later stages, suggesting another source of supernumerary *neurod*+ cells. Analysis of the cell proliferation revealed that activation of *hs:gsc* at 36 or 42 hpf dramatically increased the rate of mitosis in TA cells (Fig. 3*K*), likely accounting for increased numbers of TA cell expression of *ngn1* and *neurod* (Figs. 2*F* and 3*I*). In contrast, activation of *hs:gsc* at 22 hpf reduced the rate of proliferation among TA cells (Fig. 3*K*). Thus, activation of *hs:gsc* increases the number of TA cells by different mechanisms at different stages: Gsc increases the rate of neuroblast delamination during early stages of neurogenesis, whereas it increases the rate of proliferation in TA cells during later stages of neurogenesis. Activation of *hs:gsc* did not alter the rate of proliferation in the otic epithelium (Fig. S7*D*). *gsc* mutants showed

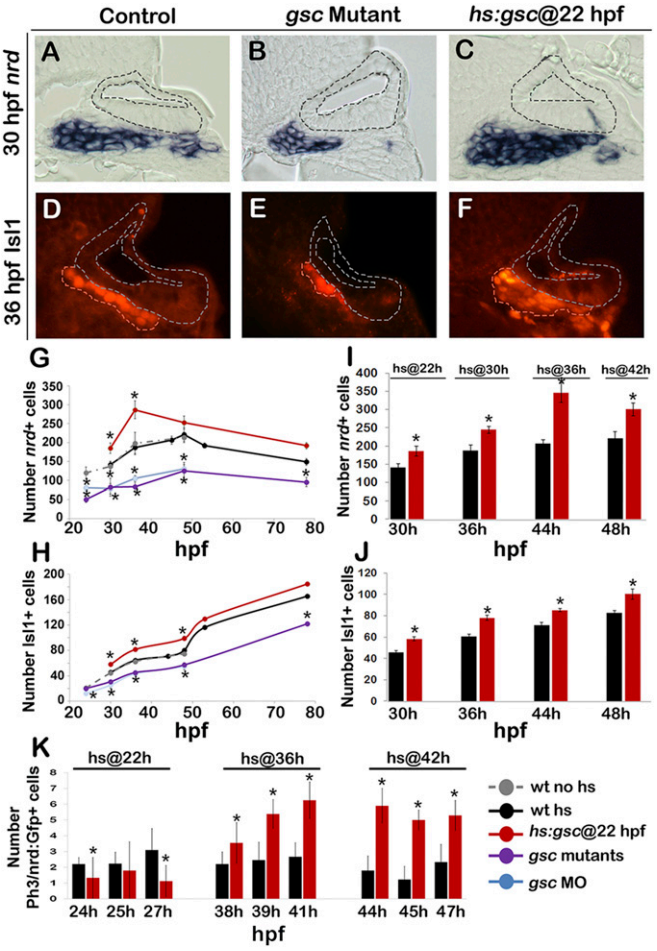


**Fig. 3.** Effects of *Gsc* on later stages of SAG development. (*A*–*F*) Cross-sections passing through the utricular sensory epithelium (dorsal up, medial left) in controls, *gsc* mutants, and *hs:gsc* embryos showing expression of *nrd* (*A*–*C*) or Isl1 (outlined in orange, *D*–*F*). The otic epithelium is outlined in all images. (Magnification: *A*–*F*, 640×.) (*G*–*J*) Mean and SD of the total number of *nrd*+ (*G* and *I*) or Isl1+ (*H* and *J*) cells for the genotypes indicated in the color key at times presented on the *x* axes. *nrd*+ cells were counted on serial sections ($n$ = 3–5), and Isl1+ cells were counted on whole mounts for time points between 30 and 48 hpf ($n$ = 10–17) and on serial sections for 53 and 78 hpf ($n$ = 2–3). (*K*) Means and SD of the total number of Phospho-Histone H3 (pH3)+ cells within the *nrd:Gfp*+ domain (which marks TA cells) at the indicated times in control and *hs:gsc* embryos. Embryos were heat shocked at the indicated times. Asterisks indicate statistically significant differences compared with control embryos ($P < 0.05$).

normal proliferation in the otic epithelium and in TA cells at all stages (Fig. S7*E*).

Despite the initial surge in *neurod*+ cells following activation of *hs:gsc* at 36 or 42 hpf, the number of *neurod*+ TA cells subsequently returned to the level seen in control embryos by 78 hpf (Fig. S7*A*). The decline in TA cells occurred concomitantly with a corresponding increase in the number of mature Isl1+ neurons (Fig. S7*B*).

*gsc* loss of function and overexpression led to a modest increase in the rate of apoptosis among hair cells and mature neurons (Fig. S7*F*). The elevated cell death possibly reflects the detrimental effects of altering epithelial integrity or nonautonomous effects of *gsc* function (see *Discussion*).

**Cooperation Between *Gsc* and *Ngn1* in Regulating EMT.** We noted that the ability of *Gsc* to promote EMT appeared to be restricted to the otic floor near the domain of *ngn1* expression. This prompted us to examine the role of *ngn1* in EMT. In *ngn1*

morphants, the number of *ngn1*+ cells that accumulated outside the otic vesicle was severely reduced (Fig. S8*A*), although a small number of delaminated cells was still observed. The fate of these cells is unclear, but they are unable to continue SAG development, as *ngn1* morphants produce no TA cells or mature SAG neurons. The number of delaminated cells nearly doubled in *ngn1* morphants following activation of *hs:gsc* but remained far below normal (Fig. S8 *B* and *C*). These data suggest that *Gsc* provides otic cells with a limited capacity for undergoing EMT in the absence of proper fate specification, but the capacity for delamination is strongly enhanced by *ngn1*. To test this further, we tested the effects of simultaneous overexpression of *gsc* and *ngn1*. Coactivation of *hs:ngn1* and *hs:gsc* resulted in additive increases in the number of *neurod*+ TA cells and mature SAG neurons by 30 hpf, and these increases persisted through at least 48 hpf (Fig. S8 *D–I*). Interestingly, activation of *hs:ngn1* induced ectopic *neurod*+ neuroblasts in the medial wall of the otic vesicle, but these neuroblasts were not observed to undergo delamination (Fig. S8*F*). In contrast, coactivation of *hs:ngn1* and *hs:gsc* appeared to promote delamination of ectopic *neurod*+ neuroblasts from the medial wall (Fig. S8*G*). Thus, *ngn1* and *gsc* synergize to promote EMT in the otic floor and to a lesser degree the medial wall. However, the ability to promote neurogenesis and delamination from ectopic sites was quite limited, suggesting that other regional factors act to oppose these functions in nonneurogenic regions.

**Pax2a Opposes *Gsc* Function in the Otic Vesicle.** We hypothesized that *pax2a*, which is expressed in the medial half of the otic vesicle, acts to oppose *gsc* function and block EMT. Pax2 has been shown to stabilize the otic epithelium during placodal stages in zebrafish, chick, and mouse (17, 18, 32, 33), raising the possibility that this function persists after expression becomes restricted to the medial wall of the otic vesicle (Fig. 4*A*). We therefore examined the functional relationship between *pax2a* and *gsc* in the otic vesicle. Normally, *pax2a* expression abuts but does not overlap the neurogenic domain in the otic floor. In *gsc* mutants, *pax2a* expression expanded laterally into the neurogenic domain, albeit at a relatively low level (Fig. 4 *B* and *G*), whereas activation of *hs:gsc* caused the domain of *pax2a* to recede slightly from the otic floor in regions near the sensory maculae (Fig. 4 *C* and *G*). Conversely, in *pax2a* mutants, the domain of *gsc* expression showed a weak medial expansion, whereas activation of *hs:pax2a* completely eliminated *gsc* expression within 2 h (Fig. 4 *D–F* and *H*). These data suggest that *gsc* and *pax2a* mutually repress each other's expression in the otic floor, with an especially prominent role of *pax2a* in repressing *gsc*. Next we examined whether *pax2a* function affects neurogenesis or EMT in the otic vesicle. Loss of *pax2a* function did not alter *ngn1* expression in the otic epithelium yet transiently increased the number of delaminated *ngn1*+ neuroblasts at 24 hpf (Fig. 4 *J* and *R*), consistent with the observed expansion of *gsc* expression in these embryos (Fig. 4 *E* and *H*). However, the number of delaminating cells in *pax2a* mutants subsequently fell to less than half of normal at 27 and 30 hpf (Fig. 4*R*). Consistent with dynamic changes in delamination, accumulation of TA cells and mature neurons was initially elevated in *pax2a* mutants but subsequently returned to normal after 30 hpf (Fig. 4 *T* and *U*). The later decline probably reflects sporadic cell death in otic neurons and epithelia as previously noted in zebrafish and mouse mutants lacking Pax2 (33–35). In contrast to the effects of disrupting *pax2a*, activation of *hs:pax2a* at 22 hpf strongly suppressed delamination of *ngn1*+ neuroblasts by 23–24 hpf (Fig. 4 *K* and *S*), consistent with loss of *gsc* expression (Fig. 4*F*). Accumulation of TA cells and mature SAG neurons was also severely impaired following activation of *hs:pax2a*, and these deficiencies persisted through at least 48 hpf (Fig. 4 *T* and *U*). Importantly, coactivation of *hs:gsc* and *hs:pax2a* at 22 hpf completely masked the effects of *hs:gsc*, causing a phenotype similar to activation of *hs:pax2a* alone: Specifically, neuroblast delamination was strongly suppressed (Fig. 4 *M* and *S*), and there was a lasting deficit in accumulation of TA cells and mature SAG neurons (Fig. 4 *T* and *U*). Thus, in addition to repressing *gsc* transcription, Pax2a antagonizes transgenic Gsc activity.

EMT is typically induced by repression of genes encoding Cadherins. We therefore surveyed expression of various *cadherin* genes in relation to *gsc* and *pax2a* function in the otic vesicle. During normal development, the E-cadherin gene *cdh1* is expressed throughout the otic vesicle, but expression levels varied markedly in the otic floor, with low-expressing cells potentially corresponding to cells undergoing EMT (Fig. 5*A*). In *gsc* mutants, *cdh1* was expressed at uniformly high levels throughout the otic floor (Fig. 5*B*), whereas activation of *hs:gsc* at 22 hpf caused global down-regulation of *cdh1* in the otic epithelium (Fig. 5*C*). The opposite relationship was seen with regard to Pax2a function: *pax2a* mutants showed little change in *cdh1* expression, although levels appeared slightly reduced in the otic floor (Fig. 5*D*). Activation of *hs:pax2a* caused substantial up-regulation of *cdh1* throughout the otic vesicle, including uniformly high expression in the otic floor (Fig. 5*E*). Coactivation of *hs:pax2a* and *hs:gsc* led to uniformly high expression of *cdh1* throughout the otic vesicle, similar to activation of *hs:pax2a* alone (Fig. 5 *E* and *F*). Changes in the percentage of cells in the otic floor expressing *cdh1*+ cells, determined by counting cells in serial sections, confirmed the above trends (Fig. 5*G*). Overall, these results suggest that *Gsc* and Pax2a have opposing effects on tissue architecture mediated in part by differential regulation of *cdh1* transcription.

Global loss of E-cadherin transcription does not lead to widespread cell dispersal in *hs:gsc* embryos. This prompted us to analyze the expression of other *cadherin* genes that might have redundant functions in the otic vesicle. Indeed, expression of *cdh2* remained unaffected in the otic vesicle upon loss of function or overexpression of *gsc* and/or *pax2a* (Fig. S9 *A–F*). *Cdh11* is expressed in the nonneurogenic regions of the otic vesicle such as the medial and lateral walls (Fig. S9*G*) and did not show any changes in *gsc* mutants or *hs:gsc* embryos (Fig. S9 *H* and *I*). However, *cdh11* transcript was lost from part of the medial wall in *pax2a* mutants, whereas activation of *hs:pax2a* induced *cdh11* expression in ectopic locations including the otic floor (Fig. S9 *J–L*). Conceivably, *cdh11* also helps to mediate Pax2a's role in stabilizing epithelial integrity. Cdh6 is predominantly expressed in the delaminated otic neuroblasts in the TA pool (Fig. S9*M*). In keeping with the effects of *gsc* on delamination, *gsc* mutants had fewer *cdh6*+ cells outside the otic vesicle and *gsc* overexpression increased accumulation of *cdh6*+ cells in the TA pool (Fig. S9 *N*, *O*, and *S*). In contrast, overexpression of *pax2a* reduced the number of *cdh6*+ otic neuroblasts outside the ear and suppressed the effects of activating *hs:gsc* (Fig. S9 *Q–S*). *pax2a* mutants showed a statistically normal number of *cdh6*+ neuroblasts at 24 hpf (Fig. S9 *P* and *S*), possibly because elevated cell death counterbalances the transient spike in neuroblast delamination seen at 24 hpf in these embryos (Fig. 4*R*).

## Discussion

Delamination from the otic vesicle is a vital step in otic neurogenesis that has heretofore been described only at the morphological level. Here we elucidate a molecular mechanism for this process (Fig. 5*H*). First, we describe a role for the organizer gene *gsc* in promoting delamination of neuroblasts from the otic vesicle. Loss of *gsc* function impairs delamination of SAG neuroblasts and leads to a significant loss of mature SAG neurons, whereas misexpression of *gsc* enhances neuroblast delamination and increases the size of the mature SAG. Second, Gsc's ability to promote EMT requires coexpression of *ngn1* as a parallel output of Fgf signaling. Comisexpression of *gsc* and *ngn1* stimulates neuroblast delamination from ectopic sites within the otic vesicle. Third, we document a role for Pax2a in stabilizing the

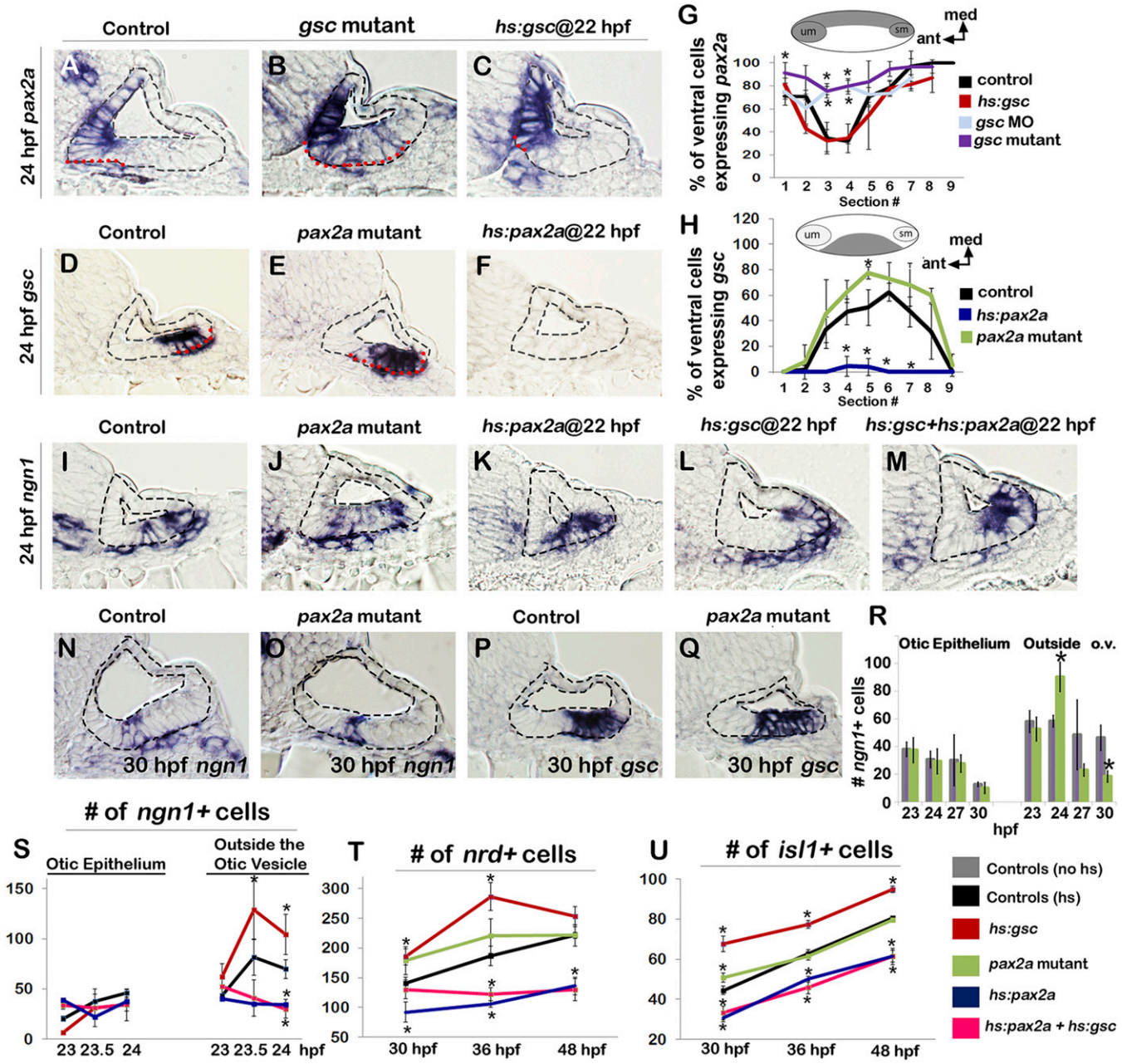


**Fig. 4.** Pax2a opposes the function of Gsc in the otic epithelium. (*A–F*) Cross-sections (dorsal up, medial left) passing through the widest part of the neurogenic domain of the otic vesicle just posterior to the utricular macula showing expression of *pax2a* or *gsc* at 24 hpf (outlined in red) in embryos with indicated genotypes. Control and transgenic embryos were heat shocked at 22 hpf. The otic epithelium is outlined black in each image. (*G* and *H*) Means and SD of the percentage of cells expressing *pax2a* or *gsc* in successive sections through the otic floor in the embryos with indicated genotypes. Data were obtained by counting the number of stained and unstained cells in each section ($n$ = 3–4 specimens). Illustrations of typical domains of *pax2a* and *gsc* (medial up, anterior left) are provided above each graph to help clarify spatial patterns within each section of the otic floor. (*I–M*) Expression of *ngn1* at 24 hpf in embryos with indicated genotypes. Transgenic embryos were heat shocked at 22 hpf. (*N–Q*) Expression of *ngn1* (*N* and *O*) and *gsc* (*P* and *Q*) in controls and *pax2a* mutants at 30 hpf. (*R–U*) Means and SD of the total number of *ngn1*+ cells inside the otic epithelium or outside the otic vesicle (*R* and *S*; counted on serial sections, $n$ = 3–4), *nrd*+ TA cells (*T*; counted on serial sections, $n$ = 3–4) and Isl1+ cells (*U*; counted on whole mounts, $n$ = 6–12). Control (hs) and transgenic embryos were heat shocked at 22 hpf and fixed at time points indicated. Asterisks indicate significant differences compared with control embryos ($P < 0.05$). *Hs:gsc+hs:pax2a* embryos were significantly different from *hs:gsc* embryos at all time points but showed no statistical difference compared with *hs:pax2a* embryos. (Magnification: All images, 640×.)

otic epithelium in opposition to Gsc. Pax2a not only represses *gsc* transcription, but it also suppresses Gsc protein function and blocks EMT. The opposing activities of Pax2a and Gsc correlate with their differential regulation of the *cdh1*, which is down-regulated in delaminating neuroblasts in zebrafish as well as mouse (36).

In this model, distinct regulation of *ngn1* and *gsc* assures orderly delamination coupled with ongoing renewal of neuroblasts within the otic epithelium: As *gsc*+ neuroblasts delaminate, adjacent neuroblasts presumably move into the *gsc* domain in preparation for their own EMT. In early stages of neurogenesis, the domain of *ngn1* expands, allowing replacement of cells lost

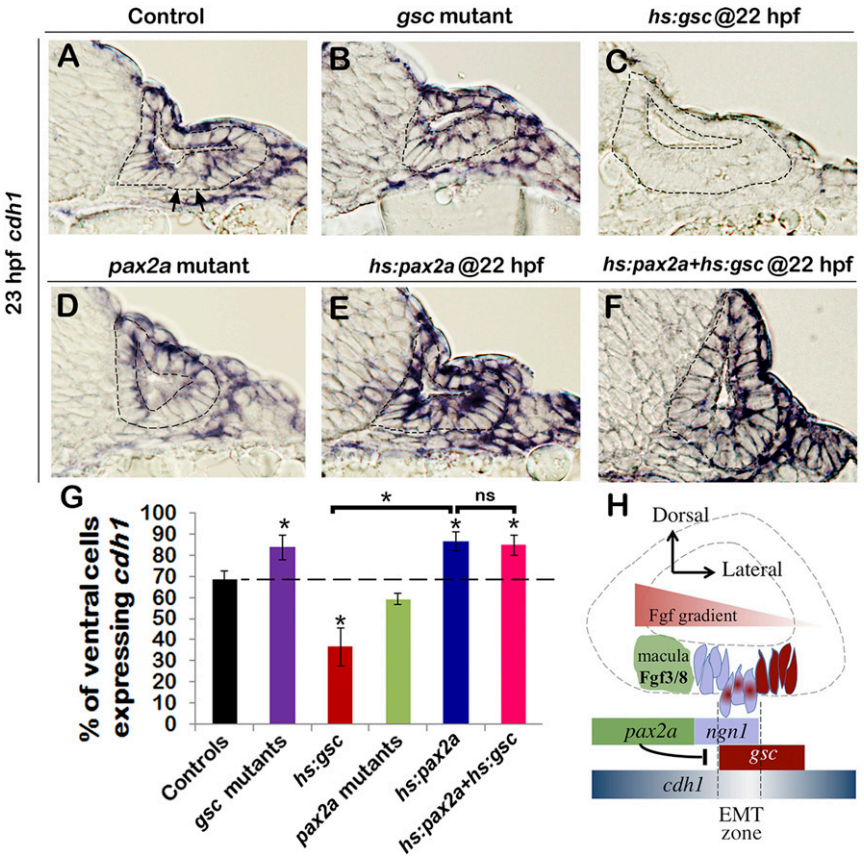


**Fig. 5.** *Gsc* and Pax2a differentially regulate *cdh1*. (*A–F*) Cross-sections passing through the neurogenic domain of the otic vesicle just posterior to the utricular macula showing *cdh1* expression at 23 hpf in embryos with indicated genotypes. The otic epithelium is outlined in each image. Arrows in *A* indicate cells with very low *cdh1* expression interspersed with cells showing high *cdh1* expression. (Magnification: *A–F*, 640×.) (*G*) Means and SD of the percentage of cells in the otic floor expressing *cdh1* in the embryos with indicated genotypes. Data were obtained by counting the number of stained and unstained cells in serial sections ($n$ = 3–4). Transgenic embryos were heat shocked at 22 hpf. Asterisks indicate significant differences between groups indicated by brackets or compared with control embryos ($P < 0.05$). (*H*) A model for regulation of epithelial tissue dynamics during otic neurogenesis. See *Discussion* for details.

through EMT. Eventually Fgf levels rise to block further *ngn1* induction (3), terminating the ability to replenish neuroblasts as they delaminate. This mechanism is reminiscent of Gsc's role in driving cellular dynamics and replenishment in the vertebrate organizer (19–22). An important goal of future research will be to conduct detailed cell-labeling experiments to elucidate patterns of epithelial rearrangement implied in our current study.

In addition to promoting EMT, overexpression of *gsc* had unexpected stage-specific effects on proliferation of TA cells. When activated at 22 hpf, *hs:gsc* caused a slight decrease in proliferation in the TA pool. This is understandable, as *hs:gsc* causes virtually all *ngn1*+ neuroblasts to delaminate at once, temporarily disrupting the normal steady flow of cycling progenitors into the TA pool. The sudden bolus of TA cells would then continue to develop synchronously and shift the population mean toward a postmitotic state, reducing the overall rate of proliferation. In contrast, activation of *hs:gsc* at 36 hpf or later caused a dramatic increase in proliferation of TA cells (Fig. 3*K*). The mechanistic basis for this is unclear but could reflect the changing status of Fgf signaling during successive stages of SAG neurogenesis (3, 12). During early stages of otic vesicle development, the level of Fgf signaling is relatively low, which stimulates specification of neuroblasts in the otic epithelium but is not sufficient to affect development of TA cells. As development proceeds, mature SAG neurons begin to accumulate and express *fgf5*, which eventually exceeds an upper threshold to terminate specification of neuroblasts in the otic epithelium. Elevated Fgf5 also delays terminal differentiation and promotes proliferation of TA cells. We speculate that forced expression of *gsc* in TA cells reinforces this effect of Fgf5, thereby increasing the TA pool disproportionately at later stages. This does not reflect a normal function of *gsc*, as it is not normally expressed in TA cells. Indeed, proliferation of TA cells was normal at all stages in *gsc* mutants (Fig. S7*E*). Further studies will be required to rigorously test the relationship between *gsc* and *fgf5* during later stages of otic development.

**Conservation and Diversity of *Gsc* Function.** The function of *gsc* in the zebrafish inner ear is likely to be conserved in other vertebrates. In mouse, *Gsc* is expressed in the developing otocyst in a pattern similar to that in zebrafish (23, 29), although its function has not been investigated. Loss of *Gsc* function in humans causes SAMS syndrome (syndrome of short stature, auditory canal atresia, mandibular hypoplasia, and skeletal abnormalities), characterized by mandibular hypoplasia similar to that seen in zebrafish *gsc* mutants, as well as loss of the auditory canal. These defects reflect deficiencies in neural crest-derived pharyngeal arches 1 and 2, known sites of *Gsc* expression, but it is unknown whether auditory neurons are also affected. Although a recently reported human chromosomal deficiency spanning *Gsc* causes auditory neuropathy, the deficiency also removes other genes that potentially affect the trait (37). Thus, additional studies are needed to clarify the role of *Gsc* in otic neurogenesis in mammals.

Interestingly, the role of Gsc in otic neurogenesis in zebrafish appears similar to the role of Gsc in regulating the stomatogastric nervous system (SNS) in *Drosophila*. SNS neuroblasts in

fly initially form in the foregut epithelium and subsequently delaminate and migrate significant distances to form the equivalent of vertebrate enteric neurons. Epithelial SNS neuroblasts express *Gsc*, and delamination is strongly impaired in *Gsc* mutants (38, 39). Additionally, delamination requires Egfr and the RAS–MAPK pathway (40, 41). Together, these findings suggest that a broadly conserved pathway, acting through RAS–MAPK and *Gsc*, functions to localize neuroblast delamination in these widely divergent species.

In addition to *gsc*, it is likely that additional factors regulate EMT in the otic vesicle. We note that neuroblasts normally begin to delaminate from the otic epithelium by 17 hpf, several hours before the onset of *gsc* expression (Fig. 1), and delamination is not completely lost in *gsc* mutants (Fig. 2*G*). A number of transcription factors known to regulate EMT in other tissues, including Snail and Zeb proteins, are also expressed in the otic vesicle at appropriate stages (42–44). These might help promote delamination from the otic vesicle, but functional studies are yet to be reported.

**Pax2 as an Epithelial Stabilizer.** Pax2 appears to coordinate cell fate specification and epithelial integrity in several contexts. In zebrafish, combinatorial knockdown of redundant genes *pax2a*, *pax2b*, and *pax8* leads to progressive dispersal of otic cells soon after formation of the otic vesicle (18). Similarly, loss of both *Pax2* and *Pax8* in mouse impairs placode invagination and severely reduces otic vesicle size, apparently due to abnormal cell migration (33). Studies in chick show that Pax2 is required for proper expression of NCAM and *N*-cadherin to stabilize epithelial integrity during placode invagination (17). A continuing role in epithelial maintenance at later stages of otic development might explain why mouse and zebrafish embryos lacking Pax2 or Pax5 function show elevated cell death in the otic vesicle, especially in sensory epithelia (34, 35). Similarly, Pax2 plays a role in epithelial maintenance during kidney development. Mouse Pax2 mutants display severe renal defects resulting from loss of epithelial structure in the nephric duct, accompanied by formation of irregular outgrowths and increased cell motility (45, 46).

**Regulation of Cadherin Dynamics.** The functions of *Gsc* and Pax2a counter each other in regulating the level of *E-cadherin* (*cdh1*) transcription (Fig. 5 *A*–*F*). E-cadherin is classically associated with epithelia, and its down-regulation is a common signature of EMT. Hence the ability of Pax2a to totally suppress the effects of *Gsc* can be explained partly through its ability to maintain *cdh1* expression. However, this mechanism is likely not sufficient. Activation of *hs:gsc* down-regulates *cdh1* throughout the otic vesicle yet does not induce widespread dispersal of the otic epithelium. This is probably because other cell adhesion molecules like *cdh2* and *cdh11* are coexpressed in the otic epithelium and are not affected by *Gsc* activity. The physical arrangement and functional relationships between coexpressed cell adhesion molecules remain poorly understood aspects of epithelial structure, but partial redundancy likely explains the limited effects of *Gsc* activity.

Another factor limiting *Gsc*'s ability to promote EMT is the requirement for coexpression of Ngn1. These factors probably regulate different subsets of genes to facilitate EMT. *Gsc* acts as a transcriptional repressor (47–50), likely explaining its ability to down-regulate *cdh1* in the otic vesicle (Fig. 5*C*) as well as in a diverse array of aggressive metastatic cancers in which *Gsc* promotes EMT (27, 28, 51). In contrast, Ngn1 acts predominantly as a transcriptional activator. Relevant targets of Ngn1 might include factors that regulate f-actin dynamics or proteases that degrade basement membrane. All of these processes are potentially coordinated under the combinatorial control of *Gsc* and Ngn1 to ensure a robust EMT response.

EMT is typically associated with Cadherin switching. For example, *cdh6* is up-regulated in neuroblasts after delamination, with weak expression first appearing in scattered cells within the otic epithelium (Fig. S9). Such switching may help weaken epithelial junctions and/or inhibit re-epithelialization of neuroblasts after delamination, while facilitating collective migration. Interestingly, the role of specific Cadherins often differs according to context. For example, *cdh11* is often associated with mesenchymal cells (52, 53) yet is expressed in the most stable parts of the otic epithelium in zebrafish (Fig. S9). Conversely, *cdh6* is expressed in migrating otic neuroblasts in zebrafish, whereas it marks premigratory neural crest in chick ectoderm and must be down-regulated to allow neural crest delamination (54, 55). The otic vesicle promises to be a useful model for future functional studies to determine how diverse cell adhesion molecules interact and contribute to tissue architecture and dynamics.

## Materials and Methods

**Fish Strains and Developmental Conditions.** All adult fish were maintained in a facility inspected and approved by the Institutional Animal Care and Use Committee (IACUC). Wild-type embryos were derived from the AB line. Transgenic lines used in this study include *Tg(hsp70:fgf8a)*$^{x17}$ (56), *Tg(hsp70l:dnfgfr1-EGFP)*$^{pd1}$ (57), *TgBAC(neurod:EGFP)* (58), *Tg (hsp70:pax2a)*$^{x23}$ (59), and (lines produced for this report) *Tg(hsp70:gsc)*$^{x58}$ and *Tg(hsp70:ngn1)*$^{x28}$. Transgenic lines are named in the text as *hs:fgf8*, *hs:dnfgfr1*, *nrd:GFP*, *hs:pax2a*, *hs:gsc*, and *hs:ngn1*, respectively. Mutant lines *gsc*$^{x59}$ and *pax2a* $^{tu29a}$ (60) were used for loss of function analysis. Homozygous mutants were identified by characteristic morphological changes. Embryos were maintained at 28.5 °C (except where noted) and staged accordingly to standard protocols (61). PTU (1-phenyl 2-thiourea, 0.3 mg/mL; Sigma) was added to block pigment formation.

**Gene Misexpression and Morpholino Injections.** To activate the heat shock transgenes, heterozygous carriers were incubated in a water bath at 39 °C for 60 min (except where noted). After heat shock, embryos were kept at 33 °C until the fixation. At least 15 embryos were observed for each time point. Transgenic carriers were identified by characteristic phenotypes when available or by PCR genotyping as previously described (62). Primer sequences are as follows (5′–3′): *hs:gsc*, GCAATGAACAGACGGGCATTTA (forward, F), GAATACACGGACACTGTTGCG (reverse, R); *hs:pax2a*, GCAATGAACAGACGGGCATTTA (F), TCTGCTTTGCAGTGAATATCCA (R). In some experiments, *ngn1* or *gsc* were knocked down by injecting embryos at the one-cell stage with 5 ng of morpholino oligomer (MO) using previously published MO sequences (1, 63).

**In Situ Hybridization and Immunohistochemistry.** Whole-mount in situ hybridization and antibody labeling were performed as previously described (64, 65). The primary and secondary antibodies used in this study are as follows: Anti-Islet1/2 (Developmental Studies Hybridoma Bank 39.4D5, 1:100), anti-GM130 (BD Transduction Laboratories 610822, 1:100), anti-ZO1 (ThermoFisher Scientific 33–9100, 1:150), anti–phospho-Paxillin pTyr118 (ThermoFisher Scientific PA5-17828, 1:50), anti–phospho-Histone H3 (EMD MILLIPORE 06–570, 1:350), and Alexa 546 goat anti-mouse or anti-rabbit IgG (ThermoFisher Scientific A-11003/A-11010, 1:50). TUNEL assay was performed by using Promega terminal deoxynucleotidyl transferase (M1871) according to the manufacturer's protocol. Whole-mount stained embryos were prepared for cryosectioning as previously described (3) and cut serially into 10-μm sections.

**Statistics.** Quantitation of cells expressing genes of interest was performed either in whole mounts ($n$ = 6–20 specimens each) or by counting cells in serial sections ($n$ = 2–4 specimens each). In experiments to test the effects of altering gene function, homozygous mutants and transgenic embryos were identified by characteristic morphological changes or PCR genotyping. Student's $t$ test was used for pairwise comparisons. Comparisons between three or more samples were analyzed by one way ANOVA and Tukey post hoc HSD (honest significant difference) test.

**ACKNOWLEDGMENTS.** This work was supported by NIH/NIDCD Grant R01-DC03806.

1. Andermann P, Ungos J, Raible DW (2002) Neurogenin1 defines zebrafish cranial sensory ganglia precursors. *Dev Biol* 251(1):45–58.
2. Ma Q, Chen Z, del Barco Barrantes I, de la Pompa JL, Anderson DJ (1998) neurogenin1 is essential for the determination of neuronal precursors for proximal cranial sensory ganglia. *Neuron* 20(3):469–482.
3. Vemaraju S, Kantarci H, Padanad MS, Riley BB (2012) A spatial and temporal gradient of Fgf differentially regulates distinct stages of neural development in the zebrafish inner ear. *PLoS Genet* 8(11):e1003068.
4. Haddon C, Lewis J (1996) Early ear development in the embryo of the zebrafish, Danio rerio. *J Comp Neurol* 365(1):113–128.
5. Hemond SG, Morest DK (1991) Ganglion formation from the otic placode and the otic crest in the chick embryo: Mitosis, migration, and the basal lamina. *Anat Embryol (Berl)* 184(1):1–13.
6. Carney PR, Silver J (1983) Studies on cell migration and axon guidance in the developing distal auditory system of the mouse. *J Comp Neurol* 215(4):359–369.
7. Kim WY, et al. (2001) NeuroD-null mice are deaf due to a severe loss of the inner ear sensory neurons during development. *Development* 128(3):417–426.
8. Jahan I, Kersigo J, Pan N, Fritzsch B (2010) Neurod1 regulates survival and formation of connections in mouse ear and brain. *Cell Tissue Res* 341(1):95–110.
9. D'Amico-Martel A (1982) Temporal patterns of neurogenesis in avian cranial sensory and autonomic ganglia. *Am J Anat* 163(4):351–372.
10. Tsuchida T, et al. (1994) Topographic organization of embryonic motor neurons defined by expression of LIM homeobox genes. *Cell* 79(6):957–970.
11. Gong Z, Hui CC, Hew CL (1995) Presence of isl-1-related LIM domain homeobox genes in teleost and their similar patterns of expression in brain and spinal cord. *J Biol Chem* 270(7):3335–3345.
12. Kantarci H, Edlund RK, Groves AK, Riley BB (2015) Tfap2a promotes specification and maturation of neurons in the inner ear through modulation of Bmp, Fgf and notch signaling. *PLoS Genet* 11(3):e1005037.
13. Raft S, et al. (2007) Cross-regulation of Ngn1 and Math1 coordinates the production of neurons and sensory hair cells during inner ear development. *Development* 134(24):4405–4415.
14. Riley BB, Phillips BT (2003) Ringing in the new ear: Resolution of cell interactions in otic development. *Dev Biol* 261(2):289–312.
15. Padanad MS, Riley BB (2011) Pax2/8 proteins coordinate sequential induction of otic and epibranchial placodes through differential regulation of foxi1, sox3 and fgf24. *Dev Biol* 351(1):90–98.
16. Hans S, Liu D, Westerfield M (2004) Pax8 and Pax2a function synergistically in otic specification, downstream of the Foxi1 and Dlx3b transcription factors. *Development* 131(20):5091–5102.
17. Christophorou NA, Mende M, Lleras-Forero L, Grocott T, Streit A (2010) Pax2 coordinates epithelial morphogenesis and cell fate in the inner ear. *Dev Biol* 345(2): 180–190.
18. Mackereth MD, Kwak SJ, Fritz A, Riley BB (2005) Zebrafish pax8 is required for otic placode induction and plays a redundant role with Pax2 genes in the maintenance of the otic placode. *Development* 132(2):371–382.
19. Blumberg B, Wright CV, De Robertis EM, Cho KW (1991) Organizer-specific homeobox genes in Xenopus laevis embryos. *Science* 253(5016):194–196.
20. Blum M, et al. (1992) Gastrulation in the mouse: The role of the homeobox gene goosecoid. *Cell* 69(7):1097–1106.
21. Cho KW, Blumberg B, Steinbeisser H, De Robertis EM (1991) Molecular nature of Spemann's organizer: The role of the Xenopus homeobox gene goosecoid. *Cell* 67(6): 1111–1120.
22. Niehrs C, Keller R, Cho KW, De Robertis EM (1993) The homeobox gene goosecoid controls cell migration in Xenopus embryos. *Cell* 72(4):491–503.
23. Gaunt SJ, Blum M, De Robertis EM (1993) Expression of the mouse goosecoid gene during mid-embryogenesis may mark mesenchymal cell lineages in the developing head, limbs and body wall. *Development* 117(2):769–778.
24. Yamada G, et al. (1995) Targeted mutation of the murine goosecoid gene results in craniofacial defects and neonatal death. *Development* 121(9):2917–2922.
25. Rivera-Pérez JA, Mallo M, Gendron-Maguire M, Gridley T, Behringer RR (1995) Goosecoid is not an essential component of the mouse gastrula organizer but is required for craniofacial and rib development. *Development* 121(9):3005–3012.
26. Parry DA, et al. (2013) SAMS, a syndrome of short stature, auditory-canal atresia, mandibular hypoplasia, and skeletal abnormalities is a unique neurocristopathy caused by mutations in Goosecoid. *Am J Hum Genet* 93(6):1135–1142.
27. Hartwell KA, et al. (2006) The Spemann organizer gene, Goosecoid, promotes tumor metastasis. *Proc Natl Acad Sci USA* 103(50):18969–18974.
28. Xue TC, et al. (2014) Goosecoid promotes the metastasis of hepatocellular carcinoma by modulating the epithelial-mesenchymal transition. *PLoS One* 9(10):e109695.
29. Vitelli F, et al. (2003) TBX1 is required for inner ear morphogenesis. *Hum Mol Genet* 12(16):2041–2048.
30. Zhao J, Yang C, Guo S, Wu Y (2015) GM130 regulates epithelial-to-mesenchymal transition and invasion of gastric cancer cells via snail. *Int J Clin Exp Pathol* 8(9): 10784–10791.
31. Nakamura N (2010) Emerging new roles of GM130, a cis-Golgi matrix protein, in higher order cell functions. *J Pharmacol Sci* 112(3):255–264.
32. Padanad MS, Bhat N, Guo B, Riley BB (2012) Conditions that influence the response to Fgf during otic placode induction. *Dev Biol* 364(1):1–10.
33. Bouchard M, de Caprona D, Busslinger M, Xu P, Fritzsch B (2010) Pax2 and Pax8 cooperate in mouse inner ear morphogenesis and innervation. *BMC Dev Biol* 10:89.
34. Kwak SJ, et al. (2006) Zebrafish pax5 regulates development of the utricular macula and vestibular function. *Dev Dyn* 235(11):3026–3038.
35. Burton Q, Cole LK, Mulheisen M, Chang W, Wu DK (2004) The role of Pax2 in mouse inner ear development. *Dev Biol* 272(1):161–175.
36. Davies D (2011) Cell-extracellular matrix versus cell-cell interactions during the development of the cochlear-vestibular ganglion. *J Neurosci Res* 89(9):1375–1387.
37. Schlade-Bartusiak K, Macintyre G, Zunich J, Cox DW (2008) A child with deletion (14)(q24.3q32.13) and auditory neuropathy. *Am J Med Genet A* 146A(1):117–123.
38. Hahn M, Jäckle H (1996) Drosophila goosecoid participates in neural development but not in body axis formation. *EMBO J* 15(12):3077–3084.
39. Hernández K, Myers LG, Bowser M, Kidd T (2015) Genetic tools for the analysis of Drosophila stomatogastric nervous system development. *PLoS One* 10(6):e0128290.
40. Forjanic JP, Chen CK, Jäckle H, González Gaitán M (1997) Genetic analysis of stomatogastric nervous system development in Drosophila using enhancer trap lines. *Dev Biol* 186(2):139–154.
41. González-Gaitán M, Jäckle H (2000) Tip cell-derived RTK signaling initiates cell movements in the Drosophila stomatogastric nervous system anlage. *EMBO Rep* 1(4): 366–371.
42. Thisse C, Thisse B, Schilling TF, Postlethwait JH (1993) Structure of the zebrafish snail1 gene and its expression in wild-type, spadetail and no tail mutant embryos. *Development* 119(4):1203–1215.
43. Thisse C, Thisse B, Postlethwait JH (1995) Expression of snail2, a second member of the zebrafish snail family, in cephalic mesendoderm and presumptive neural crest of wild-type and spadetail mutant embryos. *Dev Biol* 172(1):86–99.
44. Delalande JM, Guyote ME, Smith CM, Shepherd IT (2008) Zebrafish sip1a and sip1b are essential for normal axial and neural patterning. *Dev Dyn* 237(4):1060–1069.
45. Soofi A, Levitan I, Dressler GR (2012) Two novel EGFP insertion alleles reveal unique aspects of Pax2 function in embryonic and adult kidneys. *Dev Biol* 365(1):241–250.
46. Bouchard M, Souabni A, Mandler M, Neubüser A, Busslinger M (2002) Nephric lineage specification by Pax2 and Pax8. *Genes Dev* 16(22):2958–2970.
47. Danilov V, Blum M, Schweickert A, Campione M, Steinbeisser H (1998) Negative autoregulation of the organizer-specific homeobox gene goosecoid. *J Biol Chem* 273(1):627–635.
48. Latinkic BV, Smith JC (1999) Goosecoid and mix.1 repress Brachyury expression and are required for head formation in Xenopus. *Development* 126(8):1769–1779.
49. Yao J, Kessler DS (2001) Goosecoid promotes head organizer activity by direct repression of Xwnt8 in Spemann's organizer. *Development* 128(15):2975–2987.
50. Izzi L, et al. (2007) Foxh1 recruits Gsc to negatively regulate Mixl1 expression during early mouse development. *EMBO J* 26(13):3132–3143.
51. Taube JH, et al. (2010) Core epithelial-to-mesenchymal transition interactome gene-expression signature is associated with claudin-low and metaplastic breast cancer subtypes. *Proc Natl Acad Sci USA* 107(35):15449–15454.
52. Kimura Y, et al. (1995) Cadherin-11 expressed in association with mesenchymal morphogenesis in the head, somite, and limb bud of early mouse embryos. *Dev Biol* 169(1):347–358.
53. Hadeball B, Borchers A, Wedlich D (1998) Xenopus cadherin-11 (Xcadherin-11) expression requires the Wg/Wnt signal. *Mech Dev* 72(1-2):101–113.
54. Coles EG, Taneyhill LA, Bronner-Fraser M (2007) A critical role for Cadherin6B in regulating avian neural crest emigration. *Dev Biol* 312(2):533–544.
55. Taneyhill LA, Coles EG, Bronner-Fraser M (2007) Snail2 directly represses cadherin6B during epithelial-to-mesenchymal transitions of the neural crest. *Development* 134(8):1481–1490.
56. Millimaki BB, Sweet EM, Riley BB (2010) Sox2 is required for maintenance and regeneration, but not initial development, of hair cells in the zebrafish inner ear. *Dev Biol* 338(2):262–269.
57. Lee Y, Grill S, Sanchez A, Murphy-Ryan M, Poss KD (2005) Fgf signaling instructs position-dependent growth rate during zebrafish fin regeneration. *Development* 132(23):5173–5183.
58. Obholzer N, et al. (2008) Vesicular glutamate transporter 3 is required for synaptic transmission in zebrafish hair cells. *J Neurosci* 28(9):2110–2118.
59. Sweet EM, Vemaraju S, Riley BB (2011) Sox2 and Fgf interact with Atoh1 to promote sensory competence throughout the zebrafish inner ear. *Dev Biol* 358(1):113–121.
60. Brand M, et al. (1996) Mutations in zebrafish genes affecting the formation of the boundary between midbrain and hindbrain. *Development* 123:179–190.
61. Kimmel CB, Ballard WW, Kimmel SR, Ullmann B, Schilling TF (1995) Stages of embryonic development of the zebrafish. *Dev Dyn* 203(3):253–310.
62. Westerfield M (1993) *The Zebrafish Book: A Guide for the Laboratory Use of Zebrafish (*Brachydanio rerio*)* (University of Oregon Press, Eugene, OR).
63. Seiliez I, Thisse B, Thisse C (2006) FoxA3 and goosecoid promote anterior neural fate through inhibition of Wnt8a activity before the onset of gastrulation. *Dev Biol* 290(1): 152–163.
64. Phillips BT, Bolding K, Riley BB (2001) Zebrafish fgf3 and fgf8 encode redundant functions required for otic placode induction. *Dev Biol* 235(2):351–365.
65. Riley BB, Chiang M, Farmer L, Heck R (1999) The deltaA gene of zebrafish mediates lateral inhibition of hair cells in the inner ear and is regulated by pax2.1. *Development* 126(24):5669–5678.